Chemistry–A European Journal

Communication
doi.org/10.1002/chem.202004830

Chemistry Europe
European Chemical Societies Publishing

Polyazanes | Hot Paper |

Synthesis and Properties of Higher Nuclearity Polyazanes

Thomas Criton,[a] Debora Vilona,[a] Guy Jacob,[a] Maurice Médebielle,*[b] Elise Dumont,*[c] Lionel Joucla,*[a] and Emmanuel Lacôte*[a]

Abstract: Polyazanes (i.e., higher nuclearity homologues of hydrazines) with increasing numbers of bound nitrogen atoms (from 3 to 5), including the first pentazane ever described, were prepared by the addition of lower-order polyazanes to diazo reagents. A structure was obtained. It was shown that the polynitrogen chains adopt a helical conformation. DFT modeling shows that the arrangement persists in solution. Although the polyazanes are all reducing agents, they become less so as the number of nitrogens increases.

Many heavier p-block elements lead to electronically precise homoatomic all-σ linear chains.[1] For example, Silicon atoms can form homonuclear polysilanes, which are widely used for ceramics, as solar cells elements, etc.[2] Sulfur forms over 30 allotropes, in particular rings, but other cyclic structures with catenated sulfur atoms (with or without additional carbon atoms in the rings) also exist,[3] with important properties for biology or batteries.[4–6] On the other hand, in the second period, with the obvious exception of carbon, σ-type single-element chains atoms are generally unstable. This is the case for oxygen, whose polyatomic chains can easily decompose to release dioxygen and oxidized compounds. That is a key for ozonolysis, in which three contiguous oxygen atoms are initially part of a cycle.[7,8] Similarly, a linear four-oxygen chain has been suggested as a key intermediate in radical hydroxylations.[9]

[a] T. Criton, Dr. D. Vilona, Dr. G. Jacob, Dr. L. Joucla, Dr. E. Lacôte
Univ Lyon, Université Claude Bernard Lyon 1, CNRS, CNES
ArianeGroup, LHCEP, UMR 5278
Bât. Raulin, 2 rue Victor Grignard, 69622 Villeurbanne (France)
E-mail: lionel.joucla@univ-lyon1.fr
emmanuel.lacote@univ-lyon1.fr

[b] Dr. M. Médebielle
Univ Lyon, Université Claude Bernard Lyon 1, CNRS
CPE Lyon, INSA Lyon, ICBMS, UMR 5246
Bât. Lederer, 1 rue Victor Grignard, 69622 Villeurbanne (France)
E-mail: maurice.medebielle@univ-lyon1.fr

[c] Prof. E. Dumont
Univ Lyon, ENS Lyon, Université Claude Bernard Lyon 1, CNRS, LC, UMR 5182
46 allée d'Italie, 69364 Lyon Cedex 07 (France)
E-mail: elise.dumont@ens-lyon.fr

Supporting information and the ORCID identification numbers for the authors of this article can be found under: https://doi.org/10.1002/chem.202004830.

Hydrazines are well-known, reactivity-rich, 2N molecules, in which the two nitrogen atoms are single bonded.[10] The scenario quickly changes with higher nuclearities. Triazanes were first synthesized decades ago,[11–13] but little attention has been given to their properties.[14] Although tetrazenes, which feature both single and double-bonded nitrogen atoms, are stable moieties, only a handful of all σ tetrazanes exist,[15–18] and no higher-order polyazane has ever been reported.

We approached this field when we noticed the dearth of data regarding the reactivity of even the smallest polyazanes, triazanes. We wanted to understand how chemical properties were affected by the addition of additional nitrogen atoms in the chain, and also to extend the chemical space of higher-order polyazanes to longer chains. We report herein our initial results.

In order to get comparison points we targeted an assay of six polyazanes: two triazanes (**2a**,**b**), two tetrazanes (**3a**,**b**) and two pentazanes (**4a**,**b**). We assumed that because of all the consecutive lone pairs on the nitrogen atoms, the chains would be very electron-rich and that the all-σ chains could be stabilized by the attachment of electron-withdrawing groups. Therefore, all the target polyazanes are built similarly. They feature a terminal amine (Figure 1, top nitrogens) substituted by two alkyl groups; all other nitrogens are substituted by carbamate groups; their ω-end can be substituted either by a proton or a methyl.

Triazanes **2a** and **2b** were prepared using the Dreiding/Mayr methodology.[12,13] Dimethylamine was added to di-*tert*-butyl azodicarboxylate (DTABD) in acetonitrile at room temperature, yielding 98% of **2a**. Triazane **2b** was obtained in 86% yield upon methylation of the potassium salt of **2a** in THF/DMF (1:1) at 0 °C.

While there are methods to access the unsaturated 4N tetrazenes, for example, by reaction of a nitrene derived from a hydrazine with a diazo reagent,[19,20] or by oxidative coupling of hydrazines,[21–23] there was only one method to access the saturated fully σ-bonded tetrazanes, that is, the dimerization of captodative radicals (which can only deliver symmetric molecules).[15–18,24] One report in the literature mentioned that an α-

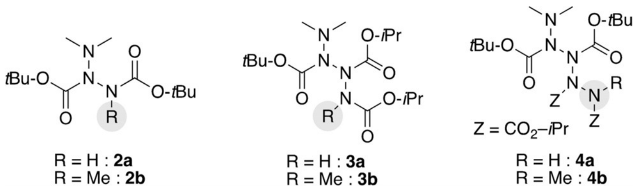

Figure 1. Target polyazanes for this work.

sulfonyl anion serendipitously added sequentially to two equivalents of an azodicarboxylate.[25] This suggested to us that hydrazinyl anions may be good reactive intermediates toward the formation of dissymmetric tetrazanes. We thus decided to prepare **3a** and **3b** by a nucleophilic addition 2N + 2N route.

Boc-protected 1,1-dimethyl hydrazine **1a** was deprotonated by potassium bis(trimethylsilyl)amide (KHMDS) in a 1:1 THF/DMF mixture at −80 °C, treated with di-isopropyl azodicarboxylate (DIAD), and quenched with acetic acid at low temperature (Scheme 1).

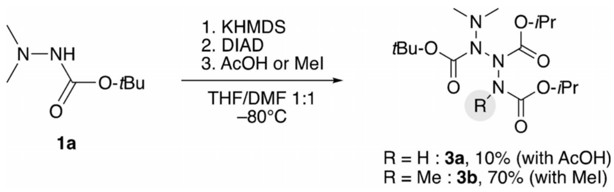

Scheme 1. Synthesis of the tetrazanes.

Tetrazane **3a** was obtained in a very poor 10% yield. It decomposed quickly at room temperature. We suspected that the decomposition was due to the presence of a proton on the chain. The methylation of the terminal NH position was achieved by trapping the intermediate anion at low temperature with MeI. Gratifyingly, **3b** was thus obtained in 70% yield, and proved more stable.

For the unknown pentazanes, a similar retrosynthetic strategy required the addition of a triazane anion to an azodicarboxylate. Triazane **2a** was first deprotonated with NaH in THF at −40 °C, and the resulting anion was reacted with DIAD (Table 1, entry 1). Unfortunately, no evolution was observed. When the solvent mix was made more polar by adding DMF, 65% of the desired pentazane **4a** was isolated after quenching the reaction at low temperature with acetic acid (entries 2 and 3). Switching to KHMDS as the base further increased the yield by nearly 10% (entry 4). Furthermore, the reaction was complete after only 15 min (entry 5). A temperature increase to −20 °C led to a loss in yield (to 59%, entry 6), while a lower temperature (−80 °C) resulted in a slower reaction (only 38% isolated yield after 15 min, entry 7). Therefore, the optimal conditions appear to be these of entry 5, likely because of the better reactivity of the potassium anion of **2a**. When the quenching agent was exchanged to methyl iodide, pentazane **4b** was isolated (76%, entry 8).

Table 1. Optimization of the reaction conditions for the synthesis of pentazanes **4a** and **4b** (concentration 0.2 M).

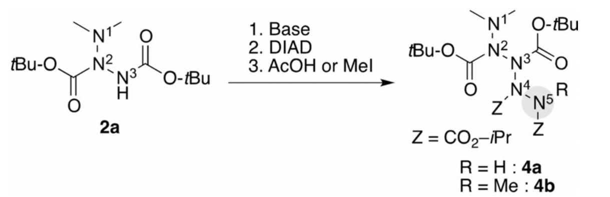

	Solvent	Base	*t* [min]	*T* [°C]	Product, Yield [%]
1[a]	THF	NaH	90	−40	–[b]
2[a]	THF/DMF (1:4)	NaH	90	−40	**4a**, 65
3[a]	THF/DMF (1:1)	NaH	90	−40	**4a**, 65
4[a]	THF/DMF (1:1)	KHMDS	90	−40	**4a**, 74
5[a]	THF/DMF (1:1)	KHMDS	15	−40	**4a**, 74
6[a]	THF/DMF (1:1)	KHMDS	15	−20	**4a**, 59
7[a]	THF/DMF (1:1)	KHMDS	15	−80	**4a**, 38
8[c]	THF/DMF (1:1)	KHMDS	15	−40	**4b**, 76

[a] Reaction was quenched with AcOH. [b] No reaction was observed. [c] Reaction was quenched with MeI.

The pentazanes proved stable over silica. They were identified by HRMS and the structure of **4a** was confirmed by X-ray diffraction (see below). They are the first examples of molecules containing 5 contiguous nitrogen atoms bound by single σ bonds. In contrast, the ^{1}H NMR spectrum of **4a** was extremely complicated due to the presence of *cis*/*trans* carbamate rotamers. We heated the samples at 80 °C to get coalescence of the signals, but this resulted in a rapid decomposition. HRMS analysis of the decomposition products suggested that the pentazane had been cleaved in a mixture of hydrazines and triazanes. We presumed that the proton at the ω position enabled this decomposition. Indeed, the methylation of said position in **4b** delivered a much more thermally stable pentazane. Its ^{1}H NMR analysis at 373 K led to a clean spectrum in which coalescence was achieved for almost all the signals.

With the array of polyazanes in hands, we could start the study of their properties, as well as how the latter change with the introduction of additional nitrogen atoms.

Crystals suitable for X-ray diffraction were obtained by slow evaporation of saturated solutions in diethyl ether at 0 °C. The X-ray structure of **2a** shows the three N atoms linked by σ bonds. Starting from the Me_2N end, the bond lengths are 1.408, and 1.383 Å. They are shorter than the bond length found in hydrazine (1.446 Å), but close to the one reported on carboxylate-protected 1,2-dimethyl hydrazine-1,2-dicarboxylate (1.386 Å).[26] The dimethylamino nitrogen displays a sp^3 hybridization, and the remaining two nitrogen atoms are sp^2 hybridized, albeit the sum of bond angles of the central atom is closer to 360° than that of the terminal sp^2 one (357.8 vs. 352.4°). This difference reflects the influence of the carboxylate groups. The dihedral angle along the N chain is 105° (Figure 2). The two carboxylate groups generate a dihedral angle of 56.9°. The minimization of the steric hindrance between the CO_2R groups explains the helical structure observed.

The X-ray structure of **4a** follows the same trends. Starting from the Me_2N end, the bond lengths are 1.400, 1.393, 1.398, and 1.386 Å. Apart from the dimethylamino nitrogen, which displays a sp^3 hybridization (average bond angle of 111.9°), all the nitrogen atoms exhibit a sp^2 hybridization. The dihedral angles along the N chain (starting from the Me_2N) are 98.2 and 86.2° respectively for the all-N dihedra, resulting in a helical arrangement of the polyazane chain, which tends to minimize the repulsion between the CO_2R groups (Figure 2).

The polyazane structures were optimized with DFT, with an implicit model accounting for acetonitrile solvation. (see Figure S1 in the Supporting Information). Interestingly, the computed most stable solution arrangements of the polynitrogen

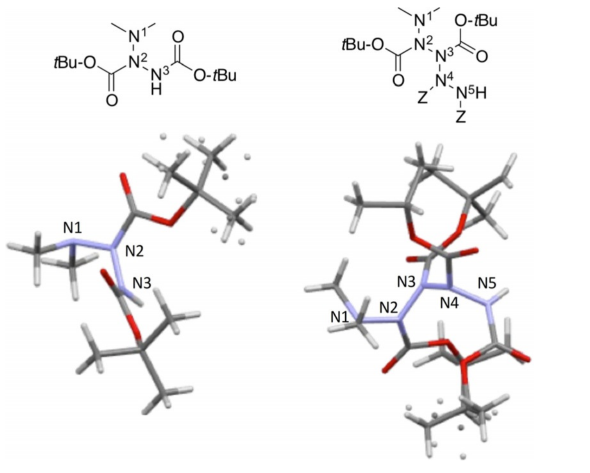

Figure 2. Structures of triazane **2a** (left) and pentazane **4a** (right). There is a slight disorder around the *tert*-butyl groups, which can freely rotate; Z = CO_2*i*Pr.

chains overlap well with those in the crystals. The calculated conformation for **3a**, for which no structure could be obtained is similar to that of **4a** with a helical arrangement. From this, we propose that the conclusions drawn for pentazanes are also valid for the tetrazanes. There is therefore a fair degree of periodicity in the polyazane family.

Hydrazines being well-known reducing agents, we examined how the redox properties are affected when additional nitrogens are linearly installed on a polyazane chain. We therefore measured the oxidation potentials of the polyazanes by cyclic voltammetry. The parent Boc-protected UDMH derivatives **1a** (featuring an N–H bond) and **1b** (where the NBoc nitrogen is also methylated) were chosen as comparison points. The values obtained are reported in the third column of Table 2.

Boc-UDMH **1a** exhibits an oxidation potential of 0.82 V (vs. SHE, entry 1). Methylation of the nitrogen increases the potential to 0.96 V (entry 2). An additional nitrogen in the chain resulted in an increased anodic peak potential (1.22 V, entry 3), which did not change by methylation of the terminal nitrogen (1.19 for **2b**, entry 4). The trend is maintained as additions of nitrogen atoms further increases the potential required for oxidation. Tetrazane **3b**, requires 1.32 V (entry 5), pentazane **4a** requires 1.43 V (entry 6) and pentazane **4b** requires 1.49 V (entry 7) to be oxidized, respectively. Tetrazane **3a** was not stable enough at room temperature to lead to significant results.

Table 2. Electrochemical data for several polyazanes.

	Compound	E^{p}_{ox} [V][a]	E^{p}_{ox} [V][b]
1	hydrazine **1a**	0.82	0.82 (=)
2	hydrazine **1b**	0.96	0.92 (−0.04)
3	triazane **2a**	1.22	1.31 (+0.09)
4	triazane **2b**	1.19	1.23 (+0.04)
5	tetrazane **3b**	1.32	1.43 (+0.11)
6	pentazane **4a**	1.43	1.53 (+0.10)
7	pentazane **4b**	1.49	1.51 (+0.02)

[a] First anodic peak potential with a glassy carbon working electrode (3 mm) with 0.1 M nBu_4NPF_6 as supporting electrolyte in MeCN; all potentials are given vs. SHE. [b] Computed absolute redox potential obtained through Born–Haber thermodynamic cycle at the M06-2X/6–31+G(d,p) level of theory, given vs. SHE (see the Supporting Information). Values in parenthesis correspond to the difference between the calculated and measured values of the first oxidation potential.

The oxidations are all irreversible, likely due to the short lifetime of the radical-cations generated. DFT calculations were therefore performed to locate the most oxidizable site in the polyazanes. The redox potential of all the molecules was estimated first through a Born-Haber thermodynamic cycle (see the Supporting Information for details).[27] Indeed, redox potentials are related to the Gibbs free energy difference between the molecules in the oxidized state (radical cation species) and the solvated molecule in the ground state (neutral molecule).

The calculated[28] redox potentials are in excellent agreement with the experimental ones (second column in Table 2, in brackets). The oxidation trend is well respected since triazane **2a** was found easier to oxidize than tetrazane **3b** and pentazane **4a** (Figure 3). We believe that the more NZ substituents we add to the molecule, the less electron density remains at the N1 atom.

For the three systems, the spin density is mostly distributed between the nitrogens N1 and N2 (Figure 4). However, DFT inspection reveals interesting differences in the populations of the radical center. For triazane **2a** and pentazane **4a**, the values identify N1 as the predominant radical center (spin coefficients 0.57 and 0.65, respectively), whereas the unpaired electron is more delocalized for **3b**. For the three systems, the inter-nitrogen distances most affected by the oxidation are that of the N1–N2 bonds, which are uniformly shortened by

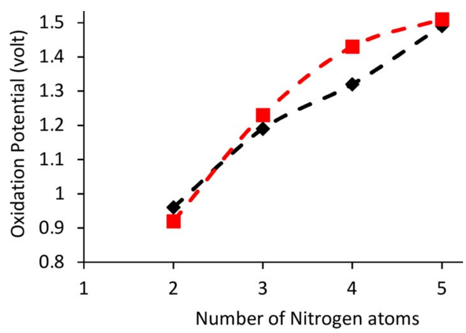

Figure 3. Evolution of the measured (◆) and calculated (■, DFT-M062X/6–31+G(d,p) level of theory) first redox potential of the polyazanes.

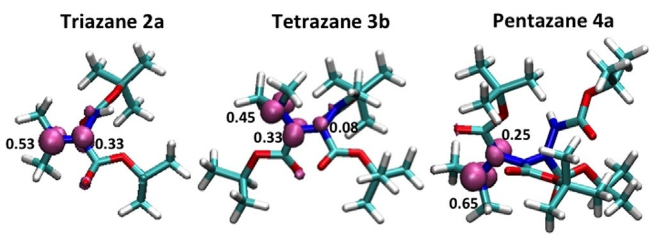

Figure 4. Cartoon representation of the optimized structures of triazane **2a**, tetrazane **3a** and pentazane **4a** in the radical cation form, optimized at the DFT-M06-2X/6–31 + G(d,p) level of theory and spin density representation (isovalue 0.10).

Table 3. Computed nitrogen–nitrogen bond lengths [Å] and hydridizations angles [°] for triazane **2a**, tetrazane **3b** and pentazane **4a**

Polyazane	**2a**			**3b**				**4a**				
Bond	N1–N2		N2–N3	N1–N2		N2–N3	N3–N4	N1–N2		N2–N3	N3–N4	N4–N5
radical cation	1.33		1.37	1.33		1.36	1.37	1.34		1.37	1.37	1.37
neutral molecule	1.39		1.38	1.40		1.36	1.37	1.40		1.37	1.37	1.37
Hybridization angle	N1	N2	N3	N1	N2	N3	N4	N1	N2	N3	N4	N5
radical cation	119.9	172.5	141.2	169.4	116.6	133.8	135.3	117.7	123.5	134.2	126.3	167.1
neutral molecule	116.3	166.0	116.2	110.9	116.6	147.1	129.0	117.5	121.2	136.3	131.3	141.3

0.06–0.07 Å upon one-electron oxidation. Conversely, the natural population analysis indicates that the nitrogen atoms sustain most of the cationic charge generated upon oxidation, with a total charge ranging between +0.5 and +0.7 a.u. (see the Supporting Information). For compounds **2a** and **4a**, the first nitrogen is the most affected, with an increase of the atomic charged by +0.37 a.u., whereas the charge of the radical cation derived from **4b** is distributed more equally over the two nitrogens, with a larger distribution of the remaining spin density contributions on the two other nitrogens and the carbonyl oxygens notably.

The calculations indicate that the most oxidizable site is the nitrogen directly connected to the dimethyl substituents, as the electron is easily removed from it, but that there seems to be a difference between the odd-numbered polyazane (**2a**, **4a**) and the even-numbered one (**3b**). Perhaps this reflects the lower stability of the tetrazanes compared to both the tri- and pentazanes, as it develops a larger positive charge density next to a withdrawing group. The nitrogen hybridization angles range between 116 and 172° (Table 3). Upon one-electron oxidation, we observed a very contrasted structural evolution as the nitrogen atom connected to the dimethyl substituents opens up widely in tetrazane **3b** (111 to 169°), but not in triazane/pentazane **2a**/**4a**, where most of the angular opening occurs at the ω-terminal nitrogen (N3 and N5, respectively).

To conclude, polyazanes are a new class of nitrogen-containing molecules that until now had not been considered as a family with similar properties. We showed that this is indeed the case, as similarly substituted polyazanes with growing numbers of linked nitrogen atoms gradually fold to form helices and become increasingly less oxidizable. Further work will focus on enlarging the chemical space accessible (e.g., to longer, or branched chains) and unearthing new properties of these new main group oligomers.

Experimental Section

Crystallographic data: Deposition number 1881825 contains the supplementary crystallographic data for this paper. These data are provided free of charge by the joint Cambridge Crystallographic Data Centre and Fachinformationszentrum Karlsruhe Access Structures service.

Acknowledgements

We thank CNES, ArianeGroup, CNRS, CPE Lyon, Université Claude Bernard Lyon 1, ENS Lyon, the SYSPROD project, the AXELERA Pôle de Compétitivité (PSMN Data Center), Institut de Chimie de Lyon, and DGA & Agence de l'innovation de défense for funding of this work. T.C. thanks DGA and CNRS for a Ph.D. stipend. D.V. thanks CNES for a postdoctoral grant.

Conflict of Interests

The authors declare no conflict of interests.

Keywords: azo compounds · molecular modeling · nitrogen · oxidation · radical cations

[1] A. L. Rheingold, *Homoatomic Rings, Chains and Macromolecules of Main-Group Elements*, Elsevier, Amsterdam, **1977**.
[2] V. B. Kumar, E. M. Leitao, *Appl. Organomet. Chem.* **2020**, *34*, e5402.
[3] B. Meyer, *Chem. Rev.* **1964**, *64*, 429–451.
[4] G. Li, S. Wang, Y. Zhang, M. Li, Z. Chen, J. Lu, *Adv. Mater.* **2018**, *30*, 1705590.
[5] N. Lau, M. D. Pluth, *Curr. Opin. Chem. Biol.* **2019**, *49*, 1–8.
[6] R. Steudel, T. Chivers, *Chem. Soc. Rev.* **2019**, *48*, 3279–3319.
[7] R. Criegee, *Angew. Chem.* **1975**, *87*, 765.
[8] C. Geletneky, S. Berger, *Eur. J. Org. Chem.* **1998**, 1625–1627.
[9] S. L. Khursan in *The Chemistry of Peroxides, Vol. 1, Part 1* (Eds.: J. F. Liebman, A. Greer), Wiley, Chichester, **2014**, pp. 197–230.
[10] E. W. Schmidt, *Hydrazine and Its Derivatives: Preparation, Properties, Applications*, 2nd ed., Wiley-Interscience, New York, **2001**. We consider here only the all-σ-bonded polynitrogen derivatives. For the most important recent advance in nitrogen chemistry, see the synthesis of the pentazolate anion: a) Y. Xu, Q. Lin, P. Wang, M. Lu, *Chem. Asian J.* **2018**, *13*, 924–928; b) Y. Xu, L. Tian, P. Wang, Q. Lin, M. Lu, *Cryst. Growth Des.* **2019**, *19*, 1853–1859; c) C. Zhang, C. Sun, B. Hu, C. Yu, M. Lu, *Science* **2017**, *355*, 374–376; d) W. Zhang, K. Wang, J. Li, Z. Lin, S. Song, S. Huang, Y. Liu, F. Nie, Q. Zhang, *Angew. Chem. Int. Ed.* **2018**, *57*, 2592–2595; *Angew. Chem.* **2018**, *130*, 2622–2625; e) B. Bazanov, U. Geiger, R. Carmieli, D. Grinstein, S. Welner, Y. Haas, *Angew. Chem. Int. Ed.* **2016**, *55*, 13233–13235; *Angew. Chem.* **2016**, *128*, 13427–13429.
[11] K.-H. Linke, H. J. Göhausen, *Chem. Ber.* **1971**, *104*, 301–306.
[12] N. Egger, L. Hoesch, A. S. Dreiding, *Helv. Chim. Acta* **1983**, *66*, 1416–1426.
[13] T. Kanzian, H. Mayr, *Chem. Eur. J.* **2010**, *16*, 11670–11677. For access to a family of completely different cyclic triazanes from N-based Lewis acids, see: a) I. Avigdori, A. Pogoreltsev, A. Kaushanski, N. Fridman, M. Gandelman, *Angew. Chem. Int. Ed.* **2020**, *59*, 23476–23479; b) A. Pogoreltsev, Y. Tulchinsky, N. Fridman, M. Gandelman, *J. Am. Chem. Soc.* **2017**, *139*, 4062–4067.
[14] A. Glowacki, V. Jeux, G. Gasnier, L. Joucla, G. Jacob, E. Lacôte, *Synlett* **2018**, *29*, 566–570.
[15] L. A. Wiles, P. Hope, *J. Chem. Soc.* **1967**, 2636–2638.
[16] W. H. Pirkle, P. L. Gravel, *J. Org. Chem.* **1978**, *43*, 808–815.
[17] B. Krumm, A. Vij, R. J. Kirchmeier, J. M. Shreeve, H. Oberhammer, *Angew. Chem. Int. Ed. Engl.* **1995**, *34*, 586–588; *Angew. Chem.* **1995**, *107*, 645–647.
[18] K. L. Martin, G. W. Breton, *Acta Crystallogr. Sect. C Struct. Chem.* **2017**, *73*, 660–666.

[19] C. Leuenberger, L. Hoesch, A. S. Dreiding, *Helv. Chim. Acta* **1981**, *64*, 1219–1233.
[20] L. Hoesch, M. Karpf, E. Dunkelblum, A. S. Dreiding, *Helv. Chim. Acta* **1977**, *60*, 816–830.
[21] A. Dhenain, C. Darwich, C. M. Sabate, D.-M. Le, A.-J. Bougrine, H. Delalu, E. Lacôte, L. Payen, J. Guitton, E. Labarthe, *Chem. Eur. J.* **2017**, *23*, 9897–9907.
[22] W. R. McBride, H. W. Kruse, *J. Am. Chem. Soc.* **1957**, *79*, 572–576.
[23] W. E. Bull, J. A. Seaton, L. F. Audrieth, *J. Am. Chem. Soc.* **1958**, *80*, 2516–2518.
[24] B. Krumm, R. L. Kirchmeier, J. M. Shreeve, *Inorg. Chem.* **1995**, *34*, 5049–5054.
[25] T. N. Balasubramaniam, N. R. Natale, *Tetrahedron Lett.* **1993**, *34*, 1099–1102.
[26] B. Doboszewski, J. McGarrah, A. Y. Nazarenko, F. da Paixao Soares, *Acta Crystallogr. Sect. E Struct. Rep. Online* **2011**, *67*, o1565.
[27] M. Laing, *J. Chem. Educ.* **2003**, *80*, 1057.
[28] K. Arumugam, U. Becker, *Minerals* **2014**, *4*, 345–387.

Manuscript received: November 4, 2020
Accepted manuscript online: December 28, 2020
Version of record online: January 26, 2021

